

Network Structures and Thermal Characteristics of $\text{Bi}_2\text{O}_3\text{-SiO}_2\text{-B}_2\text{O}_3$ Glass Powder by Sol-Gel



Peixian Li, Gecheng Yuan, Zhenghua Lu, Qian Li and Qiguang Wu

Abstract Glass powder of $\text{Bi}_2\text{O}_3\text{-SiO}_2\text{-B}_2\text{O}_3$ was prepared by Sol-Gel method, and the powder was heated to the temperature range from 200 to 800 °C to study the network structures formed during heat treatment. The effect of structures change of the glass powders on the transition temperature and sintering softening properties was analyzed. The results indicate that Bi^{3+} get into the network structure with the rising of heat treatment temperature, $[\text{BiO}_6]$ octahedral and $[\text{BiO}_3]$ triangle, $[\text{BO}_4]$ tetrahedron and $[\text{BO}_3]$ triangle connected with $[\text{SiO}_4]$ tetrahedron separately in the way of vertex connecting to build the network structures. The O1s and Bi4f binding energies increase gradually while the B1s binding energies decrease, which strengthen the stability of glass structure. This causes an increase in the transition temperature and a decrease in the wettability of the glass powder. The glass powders treated at 600 °C have excellent sintering properties. The glass transition temperature (T_g) is about 542, and the thermal expansion coefficient (25–300 °C) is close to $6.57 \times 10^{-6}/^\circ\text{C}$.

1 Introduction

$\text{Bi}_2\text{O}_3\text{-SiO}_2\text{-B}_2\text{O}_3$ glass powder is a research hot-spot of lead-free glass system. It has broad application prospects in electronic packaging, electronic paste, and so on

The original version of this chapter was revised: correct acknowledgement has now been updated. The correction to the book is available at https://doi.org/10.1007/978-981-13-5947-7_25

P. Li · G. Yuan (✉) · Z. Lu · Q. Li

School of Materials and Energy, Guangdong University of Technology, Guangdong, Guangzhou 510006, China

e-mail: gchyuan@gdut.edu.cn

P. Li

e-mail: lipeixianx@163.com

Q. Wu

Analysis and Test Center, Guangdong University of Technology, Guangzhou 510006, China

© Springer Nature Singapore Pte Ltd. 2019

Y. Han (ed.), *Physics and Techniques of Ceramic and Polymeric Materials*,

Springer Proceedings in Physics 216,

https://doi.org/10.1007/978-981-13-5947-7_24

[1]. Bi_2O_3 is an important component of bismuthate glasses. The structural properties such as coordination state and bond length of bismuth ions are the key factors affecting the structure and material properties of boron oxide and silicon oxide networks [2, 3]. Some literatures have shown that the spatial network structure of bismuthate glasses consists of Bi^{3+} with large radius and low field strength combined with a small amount of traditional glass network-forming bodies (such as B^{3+} and Si^{4+}) [4]. However, some scholars believe that Bi^{3+} will undergo polarization deformation and form a spatial network structure in the form of asymmetric $[\text{BiO}_6]$ octahedron [5]. B_2O_3 is a glass network-forming body, and its high glass forming ability is derived from a complex stacked structure, and the amorphous random network structure is formed by a B-O ring and a BO_3 triangular chain through a B-O-B link. Therefore, when Bi_2O_3 and B_2O_3 together form a glass, Bi^{3+} with high ion polarization and multiple coordination numbers is likely to form a more complex amorphous structure with a small amount of B^{3+} , and the resulting network structure will directly affect the thermal performance of the glass powder. At present, the preparation of glass powder is mostly carried out by melt quenching method, and the structure research of the glass powder prepared by the method has been reported, while the structural analysis of the glass powder prepared by the new preparation method such as the sol-gel method is rarely systematically studied, especially in the process of heat treatment during the preparation process, the structural changes of the glass powder need to be studied in depth [6–8]. Therefore, it is necessary to have an in-depth understanding of the relationship between the structural change of the glass powder and its thermal properties. In this paper, prepared by sol-gel method, a Bi_2O_3 - SiO_2 - B_2O_3 -based glass powder, the interconnection and network formation mechanism of various network groups in glass at different heat treatment temperatures was studied. Based on this, a glass network structure model was constructed and the influence of network structure changes on glass powder transformation temperature (T_g) and sintering softening characteristics was analyzed.

2 Experiment

2.1 Sample Preparation

$\text{Bi}(\text{NO}_3)_3 \cdot 5\text{H}_2\text{O}$, TEOS, H_3BO_3 , $\text{Zn}(\text{NO}_3)_2 \cdot 6\text{H}_2\text{O}$, $\text{Al}(\text{NO}_3)_3 \cdot 9\text{H}_2\text{O}$ are used as precursors; deionized water, ethanol and nitric acid are used as solvents and catalysts, respectively. According to the glass composition oxide ratio (quality percentage) 60% Bi_2O_3 , 10% SiO_2 , 20% B_2O_3 , 7% ZnO and 3% Al_2O_3 , the mass of the raw material is converted into a solution, mixed in a certain order and mechanically stirred, and the mixed solution is aged in a constant temperature water bath at 60 °C for a certain period of time to obtain a transparent wet gel. The wet gel was dried at 100 °C for 1 h in a dry box, and an appropriate amount of dry gel was selected and heat treated in a muffle furnace at 200, 400, 600 and 800 °C for 1 h and then subjected

to mechanical ball milling for 20 h to obtain a glass powder sample. Several powder samples were taken out for characterization. The remaining powders were made into a cylindrical sample for sintering test and thermal expansion performance test using a pressure tester and a specific mold. The cylindrical sample has a diameter (Φ) of 8 mm and the height (h) of 12 mm.

2.2 Sample Characterization

The morphology of the glass powder was analyzed by Hitachi S-4300N SEM and JEM-1400 TEM analyzer. The glass network structure was analyzed by ESCALAB-250 XPS, Nicolet 380 FT-IR and inVia Raman; Y- Model 2000 XRD was used to analyze the crystallization characteristics of glass powder samples at different heat treatment temperatures. The glass transition characteristics and thermal expansion characteristics of glass powder samples in various temperature ranges were tested by 3SDT-2960 DSC-TG and NETZSCH DIL402PC thermal dilatometer. The button sintering experiment is used to test the wettability of the glass powder and the matrix material, and the contact angle θ is measured according to the principle of the sessile drop method with (1).

$$\theta = 2tg^{-1}(2h \cdot d^{-1}) \quad (1)$$

where, h , d are the height and diameter of the glass after sintering, respectively.

3 Results and Discussion

3.1 Network Structure Analysis

Figure 1a shows the IR absorption spectrum of the powder after heat treatment at different temperatures. With the treatment temperature increases, the OH^{-1} or H_2O vibration in the powder decreases at 3450 and 1600 cm^{-1} [9]. The intensity of B–O bond stretching vibration peak in $[\text{BO}_4]$ at 1182 cm^{-1} decreases, while the vibration intensity of B–O–Si structure increases at 1370 cm^{-1} . It is indicated that as the heat treatment temperature increases, the $[\text{BO}_4]$ tetrahedron is connected with the $[\text{SiO}_4]$ tetrahedron apex angle to share the O atom to form the Si–O–B structure [10]. The absorption intensity caused by the vibration of the $[\text{BiO}_3]$ triangular structure at 900 and 860 cm^{-1} gradually decreases, while the vibration intensity of the Si–O–Bi structure at 670 cm^{-1} gradually increases. It shows that Bi^{3+} is gradually added to the Si–O–Si network and participates in the construction of the glass network to form the Si–O–Bi structure [11]. As $[\text{BO}_4]$ is connected to $[\text{SiO}_4]$ and Bi^{3+} ions are continuously added to the Si–O–Si network, the symmetry of the $[\text{SiO}_4]$ tetrahedron

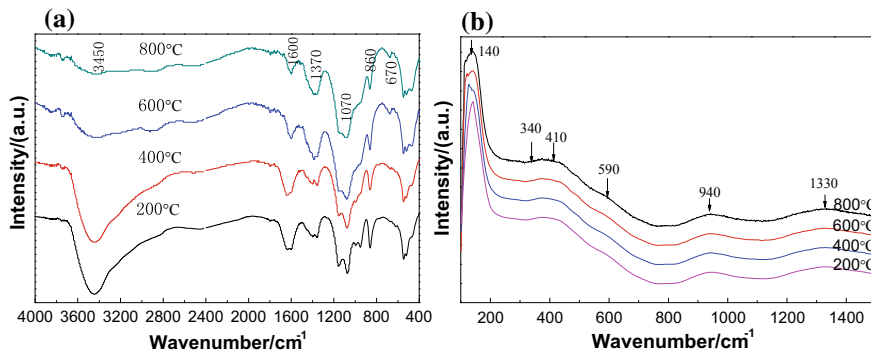


Fig. 1 IR (a) and Raman (b) spectrum of powder treated at different temperature

is destroyed, that results in absorption intensity structure of Si–O–Si asymmetric stretching vibration at 1070 cm^{-1} gradually increased.

Figure 1b shows the Raman spectrum of the powder after heat treatment at different temperatures. The most intense peaks occurred at 140 cm^{-1} , it is the characteristic vibration peak of $[\text{BiO}_6]$ octahedron and $[\text{BiO}_3]$ triangle caused by Bi^{3+} ion as a network forming body entering the glass structure [11]. The scattering peaks at $305\text{--}325$ and $410\text{--}420\text{ cm}^{-1}$ are Bi–O–Bi symmetric stretching vibration modes in $[\text{BiO}_6]$ and $[\text{BiO}_3]$, respectively [12]. As the heat treatment temperature increases, the scattering intensity of the glass powder increases at the two locations. It shows that the number of $[\text{BiO}_6]$ and $[\text{BiO}_3]$ increases with Bi^{3+} ions entering the glass network. The vibration peak near $575\text{--}590\text{ cm}^{-1}$ is mainly due to the stretching vibration of Bi–O[−] non-bridge oxygen bond in $[\text{BiO}_6]$, and temperature has little effect on Bi–O[−] non-bridged oxygen bonds in glass [13]. The scattering peak at $1250\text{--}1330\text{ cm}^{-1}$ is the stretching vibration of B–O–B in the $[\text{BO}_3]$, and the intensity of the scattering peak gradually decreases with the increase of temperature. The reason is that the temperature rise causes the $[\text{BO}_3]$ triangle to break into a chain structure, and the $[\text{BO}_3]$ triangle is connected with the $[\text{SiO}_4]$ tetrahedron apex angle to share the O atom to form the Si–O–B structure, and the vibration directed low wave direction, it is indicated that the $[\text{BO}_3]$ group may be attached to the $[\text{BiO}_6]$ or $[\text{BiO}_3]$ group with a lower wave number due to the high charge of Bi^{3+} and the strong polarization. When the symmetric stretching vibration peak of Si–O–Si in the $[\text{SiO}_4]$ is 940 cm^{-1} , the scattering peak intensity decreases with increasing temperature [11]. It shows that Bi^{3+} enters the Si–O–Si network structure and participates in the construction of the glass network. At the same time, $[\text{BO}_3]$ is connected with $[\text{SiO}_4]$, which destroys the symmetry of the $[\text{SiO}_4]$ tetrahedron, which is consistent with the IR spectrum analysis.

Figure 2a is an O1s XPS of the powder after heat treatment at $200\text{ }^\circ\text{C}$. The peak of O1s has a width of about 6 eV, which can be divided into bridge oxygen (BO) and non-bridge oxygen (NBO), and the non-bridge oxygen peak area is smaller than the bridge oxygen peak area [14]. It is indicated that the oxygen in the glass structure is mainly in the form of Si–O–Si. At the same time, part of Bi^{3+} in the glass

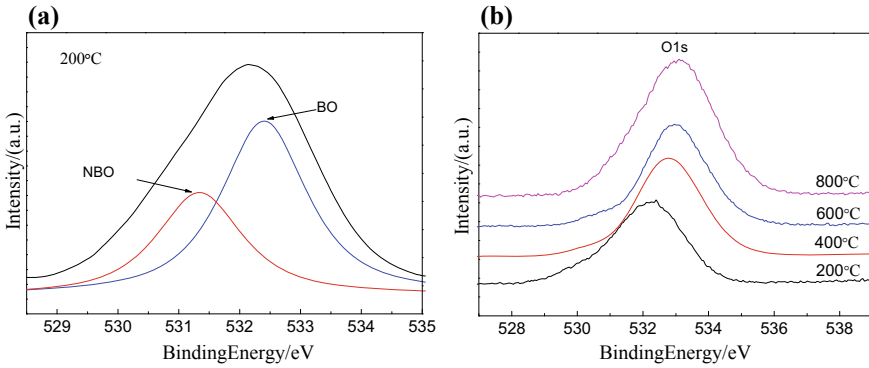


Fig. 2 O1s XPS of powder treated at 200 °C (a) and different temperature (b)

enters the glass network structure after heat treatment, and the $[\text{BiO}_6]$ or $[\text{BiO}_3]$ is connected with the $[\text{SiO}_4]$ to form Si–O–Bi. Figure 2b shows the O1s XPS of the powder after heat treatment at different temperatures. With the increase of heat treatment temperature, the electron binding energy of O1s increased from 532.3 to 533.1 eV, and the oxygen ion concentration also increased gradually, indicating that the chemical bonds formed by other atoms connected with O are large, the cations are enhanced by oxygen ion binding, and glass network structure is more compact [11, 14].

Figure 3a shows the XPS of Bi4f of powder after heat treatment at different temperatures. As the temperature increases, the binding energy of $\text{Bi}4f_{7/2}$ increases from 159.5 to 159.9 eV, and the binding energy of $\text{Bi}4f_{5/2}$ increases from 164.8 to 165.3 eV. This may be due to the increase of oxygen ion concentration in the glass. The $6s^2$ lone pair of electrons of some Bi^{3+} ions are strongly electrostatically repelled by oxygen ions, which makes the Bi^{3+} ions become Bi^{5+} ions, which reduces the electron density of Bi–O bonds [14]. In addition, since the Si–O bond length in the glass network structure is 1.61 Å, the temperature rises, and Bi^{3+} gradually enters the glass network structure, and the Bi–O bond length of the Si–O–Bi structure is between 2.2 and 2.8 Å. Therefore, the formed Si–O–Bi structure is increased in electrostatic repulsion due to the increased cation distance between silicon and germanium, and the stability of the glass network structure is enhanced.

Figure 3b shows the XPS of B1s of the powder after heat treatment at different temperatures. With increasing temperature, the binding energy of B1s decreases from 192.5 to 192.4 eV. This is probably because of the $[\text{BO}_3]$, $[\text{BO}_4]$ and $[\text{SiO}_4]$ form Si–O–B structures. Because the electronegativity of B is larger than that of O and Si, the electrons tend to shift to the large electronegative atoms which lead to the increase in the density of the electron cloud around B, the increase of the shielding effect and the decrease of the corresponding electron binding. Moreover, since the B–O bond energy is 119 kcal/mol, which is larger than the Si–O bond energy of 106 kcal/mol, the formed Si–O–B structure is more stable.

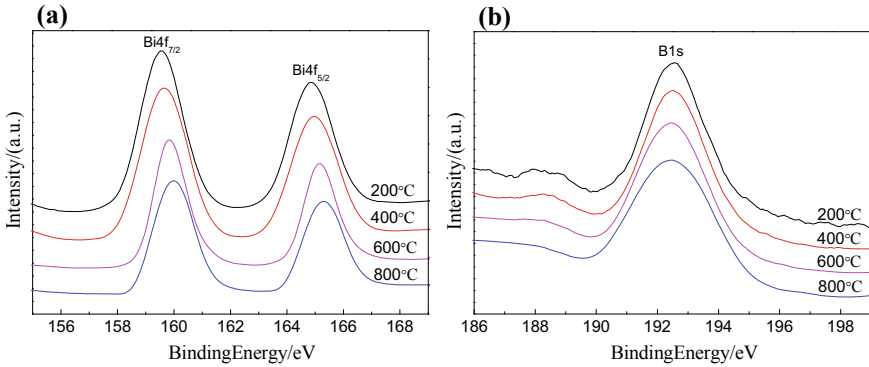
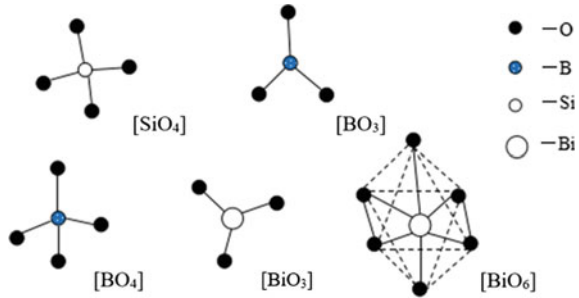


Fig. 3 Bi 4f (a) and B 1s (b) XPS of powder treated at different temperature

Fig. 4 Structural units of glass powder



The above IR, Raman spectrum and XPS analysis show that the units forming glass network structure are mainly like [BiO₆], [BiO₃], [BO₄], [BO₃] and [SiO₄] in Fig. 4. As the main component of glass, Bi₂O₃ exists first in the form of modifier in the glass network. The network structure of the glass is mainly constructed by the [SiO₄] tetrahedron in SiO₂ and the [BO₄] tetrahedron in B₂O₃ and the [BO₃] in the way of the top angle, as shown in Fig. 8.

After heat treatment at different temperatures, Bi³⁺ gradually enters the glass network, destroying the original glass network structure. The [SiO₄], [BO₄] and [BO₃] body, respectively, form a glass network structure with the formed [BiO₆] and [BiO₃] reconnected at the vertex angle. As shown in Fig. 5a, the [SiO₄], the [BO₄] and the [BO₃] are constructed with the [BiO₆] and the [BiO₃], which are connected to the top angle, respectively, as shown in Fig. 5b.

3.2 Thermal Performance

Figure 6a shows the XRD of the powders after heat treatment at different temperatures. After heat treatment at different temperatures, the diffraction peaks of the

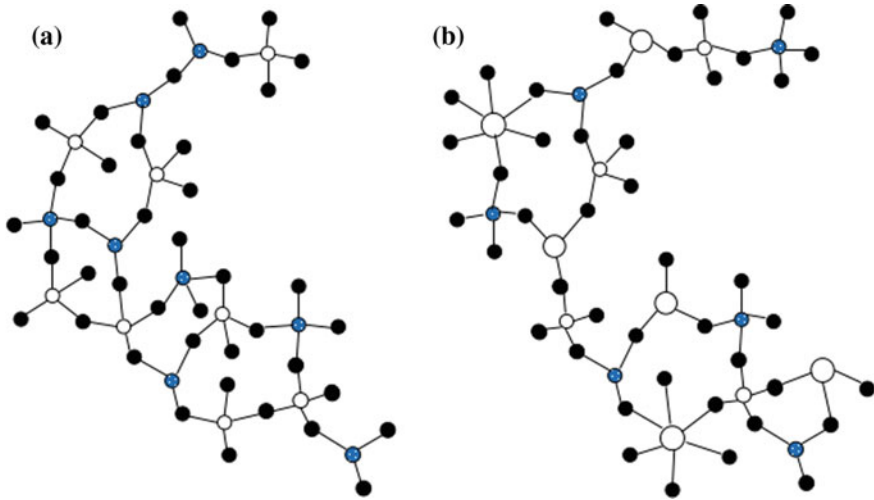


Fig. 5 Structural model of original glass (a) and glass powder after heat treatment (b)

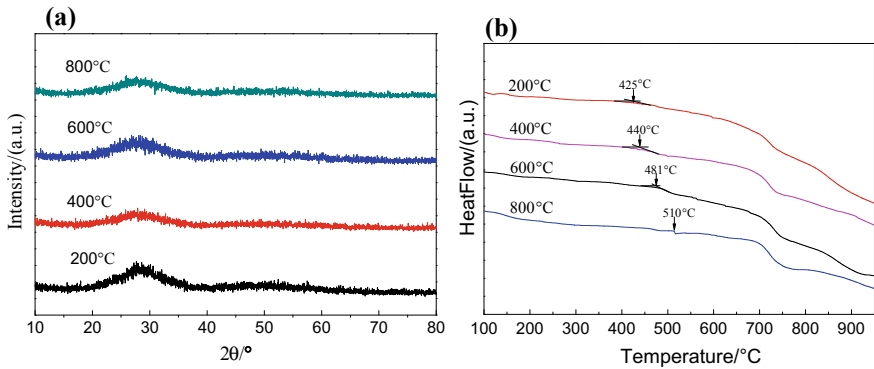


Fig. 6 XRD spectrum (a) and DSC curves (b) of powder treated at different temperature

patterns did not change significantly. It has always been characterized by the widening and dispersion characteristics of typical amorphous materials [15]. That is, the glass state powders of the system can be successfully prepared by sol-gel method.

The transition temperature (T_g) is an important characteristic temperature of glass [5]. The size of T_g is closely related to the bond strength between atoms and the network structure of glass. Figure 6b is the DSC curve of the glass powder after heat treatment at different temperatures. With the increase in heat treatment temperature, the T_g of glass powder increased from 425 to 510 °C. It shows that the network structure of glass increases gradually and the aggregation degree increases, which is corresponding to the above network structure analysis. The melting endothermic peaks of the powders after heat treated at different temperatures were between 700

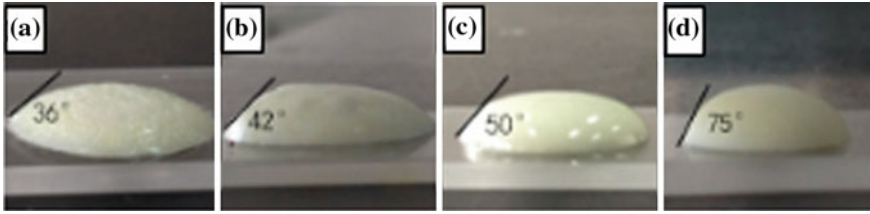


Fig. 7 Photographs showing the softening state of sintered cylindrical samples of powder treated at different temperature. **a** 200 °C; **b** 400 °C; **c** 600 °C; **d** 800 °C

and 750 °C. It is indicated that when the glass powder is sintered in this temperature range, the viscosity of the glass is insufficient to support the glass to cause a large shape change. In addition, there is no crystal exothermic peak in the whole test temperature range.

Photographs showing the softening state of sintered glass samples at 725 °C with heat-treated glass powders under different temperatures is Fig. 7. The cylindrical pattern of glass powder becomes hemispherical or even dispersed. Combined with the above DSC analysis, it is known that the inner surface of the glass powder cylinder is close to each other and bonded, increased fluidity, resulting in surface profile deformation [16]. The glass powder after the heat treatment may have better wetting with the substrate at different temperatures, sintered glass frit powder preferably wettability of 200 °C, but the surface is rough and porous after sintering, resulting in poor density. As the heat treatment temperature increases, the contact angle increases from 36° to 75°. The wettability has a certain degree of decline, but the density is increased after sintering, and the surface has a clear glass luster. Therefore, considering the comprehensive consideration, the glass powder after heat treatment at 600 °C has good wettability, density and surface gloss.

Figure 8a is the SEM morphology of the glass powder after heat treatment at 600 °C for 20 h after ball milling. The particle size of powder is less than 1 μm and mainly spherical like. Further, the glass powder is observed by TEM. As shown in Fig. 8b, the surface of the glass powder is covered with nanoparticles of about 10–20 nm [16]. This is the embodiment of colloidal particles in powder. During the gel formation process, the colloidal particles are continuously increased and grown to form a gel. After drying, the nanoparticles are stored in the glass yet. In the ball milling process, the nanoparticles are adsorbed on the surface of the glass powder and piled up layer by layer. Therefore, the specific surface area of the prepared glass powder is large, and the surface energy is higher. In the sintering process, it is beneficial to improve the fluidity and the densification of the sample. This is also reflected in the above sintering experiments.

Figure 9 is a graph showing the thermal expansion coefficient of the glass powder pattern after heat treatment at 600 °C. The curve shows an upward sharp turn near 485 °C, corresponding to the T_g , a peak occurs at about 542 °C, corresponding to the dilatometric softening point temperature of glass (T_d). The coefficient of thermal

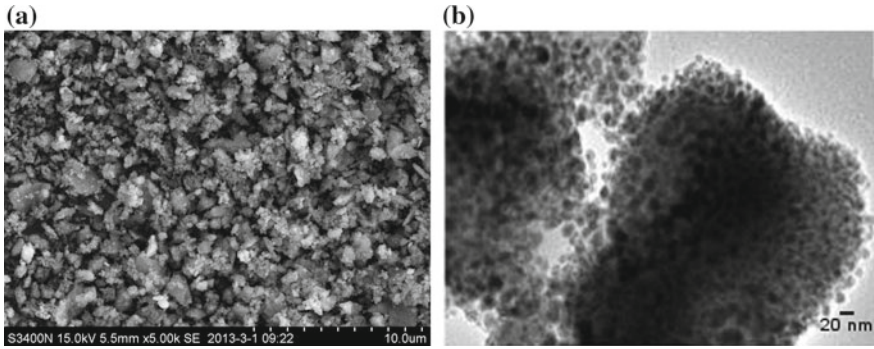
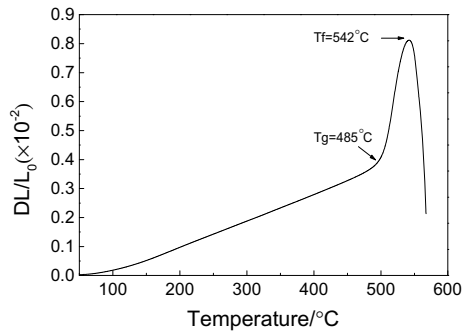


Fig. 8 SEM (a) and TEM (b) image of powder treated at 600 °C

Fig. 9 Thermal expansion curve of powder treated at 600 °C



expansion (25–300 °C) α was calculated to be about $6.57 \times 10^{-6}/^{\circ}\text{C}$. Therefore, the glass powder after heat treatment at 600 °C has a stable network structure and a low softening temperature, does not undergo crystallization during sintering, and has good wettability with the substrate, while can be applied to the sealing temperature of the base material at about 725 °C. The coefficient of thermal expansion (25–300 °C) is about $6.57 \times 10^{-6}/^{\circ}\text{C}$ for fluxing and sintering.

4 Conclusions

- (1) Within the test temperature range, as the heat treatment temperature increases, Bi^{3+} gradually enters the glass network, $[\text{BiO}_6]$ and $[\text{BiO}_3]$, $[\text{BO}_4]$ and $[\text{BO}_3]$ connected with $[\text{SiO}_4]$ separately in the way of vertex connecting to build the network structures.
- (2) The structures of Si–O–Bi and Si–O–B of glass powder form gradually during heat treatment. With the increase of heat treatment temperature, the electron binding energy of O1s and Bi4f increases and the electron binding energy of

BIs decreases gradually. Therefore, the stability of the glass network structure is enhanced.

- (3) The change of the glass powder network structure is the main reason that the T_g increases and the wettability decreases with the heat treatment temperature. The powder after heat treatment at 600 °C has good sintering performance and softening temperature. The coefficient of thermal expansion (25–300 °C) α is about $6.57 \times 10^{-6}/^\circ\text{C}$.

Acknowledgements This work was financially supported by Guangdong Provincial Natural Science Fund of China (Nos. 2006B14701003) and Guangzhou Science and Technology Project of China (Nos. 201510010034).

References

1. Y.U. Xiaojun, Z.H.U. Lihui et al., Effects of Bi_2O_3 on structure and properties of Al_2O_3 - ZnO - Bi_2O_3 - B_2O_3 low-melting glasses. *Electron. Compon. Mat.* **32**(9), 12–14 (2013)
2. H.E. Feng, D.E.N.G. Dawei, W.A.N.G. Jun, Effect of Bi_2O_3 contents on sintering property of Bi_2O_3 - ZnO - B_2O_3 system low-melting electronic sealing glass. *J. Wuhan Univ. Technol.* **31**(22), 1–4 (2009)
3. Z. Hongping, Z. Renjie, Effects of CuO on structure and heat treatment of Bi_2O_3 - B_2O_3 - ZnO glasses. *J. Ceram.* **31**(4), 569–574 (2010)
4. J. Cheng, F. Chen, S. Dai, et al., Vitreous network formation and optical characteristics of glasses within Bi_2O_3 — B_2O_3 binary system. *J. Chin. Ceram. Soc.* **41**(4), 475–479 (2013)
5. Y. Huang, Y. Li, J. Wang, et al., Network structures and characteristics of Bi_2O_3 - ZnO - B_2O_3 Ternary system glasses. *J. Chin. Ceram. Soc.* **43**(7), 998–1001 (2015)
6. S. Shruti, A.J. Salinas, G. Malavasi et al., Structural and in vitro study of cerium, gallium and zinc containing Sol-Gel bioactive glasses. *J. Mater. Chem.* **22**(27), 13698–13706 (2012)
7. J. Chen, W. Que, Y. Xing et al., Molecular level-based bioactive glass-poly (caprolactone) hybrids monoliths with porous structure for bone tissue repair. *Ceram. Int.* **41**(2), 3330–3334 (2015)
8. B.B. Das, A. Srinivassan, M. Yogapriya, et al., Sol–gel synthesis and characterization of $x\text{CuO}$ - $(1-x)\text{Bi}_2\text{O}_3$ ($0.15 \leq x \leq 0.55$) glasses by magnetic and spectral studies. *J. Non-Cryst. Solids* **427**, 146–151 (2015)
9. M. Wang., Investigation of the structure evolution process in sol–gel derived CaO - B_2O_3 - SiO_2 glass ceramics. *J. Non-Cryst. Solids* **357**, 1160–1163 (2011)
10. X. Zhu, C. Mai, M. Li, Effects of B_2O_3 content variation on the Bi ions in Bi_2O_3 - B_2O_3 - SiO_2 glass structure. *J. Non-Cryst. Solids* **388**, 55–61 (2014)
11. H. Fan, Infrared, Raman and XPS spectroscopic studies of Bi_2O_3 - B_2O_3 - GeO_2 glasses. *Solid State Sci.* **12**(4), 541–545 (2010)
12. Y. Zhang, Y. Yang, J. Zheng et al., Effects of oxidizing additives on optical properties of Bi_2O_3 - B_2O_3 - SiO_2 glasses. *J. Am. Ceram. Soc.* **91**(10), 3410–3412 (2008)
13. I. Ardelean, S. Cora, FTIR and Raman investigations of MnO - B_2O_3 - Bi_2O_3 . *Optoelectron. Adv. Mater.* **12**(2), 239–243 (2010)
14. H.W. Nesbitt, G.M. Bancroft, et al., Bridging, non-bridging free (O_2^-) oxygen in Na_2O - SiO_2 glasses. *J. Non-Cryst. Solids* **1**(357), 173–175 (2011)
15. L.E. Yingfeng, Y.U.A.N. Gecheng, L.I. Qian et al., Thermal properties of Bi_2O_3 - SiO_2 - B_2O_3 - Zn O - Al_2O_3 glass powders prepared by sol-gel method. *China Powder Sci. Technol.* **23**(1), 85–87 (2017)

16. D.I.N.G. Kanjunjie, C.H.E.N. Nan, Preparation, structures, thermal properties and sintering behaviors of B_2O_3 - SiO_2 - ZnO - BaO - Al_2O_3 glass. *J. Wuhan Univ. Technol. Mater* **31**(6), 1323–1328 (2016)